Langmuir

ARTICLE

pubs.acs.org/Langmuir

Stable Protein-Repellent Zwitterionic Polymer Brushes Grafted from Silicon Nitride

Ai T. Nguyen,[†] Jacob Baggerman,[*,‡] Jos M. J. Paulusse,[†] Cees J. M. van Rijn,[†,‡] and Han Zuilhof[*,†]

[†]Laboratory of Organic Chemistry, Wageningen University, Dreijenplein 8, 6703 HB Wageningen, The Netherlands

[‡]Aquamarijn Micro Filtration B.V., Berkelkade 11, 7201 JE Zutphen, The Netherlands

Supporting Information

ABSTRACT: Zwitterionic poly(sulfobetaine acrylamide) (SBMAA) brushes were grafted from silicon-rich silicon nitride (Si_xN_4, $x > 3$) surfaces by atom transfer radical polymerization (ATRP) and studied in protein adsorption experiments. To this aim ATRP initiators were immobilized onto Si_xN_4 through stable Si−C linkages via three consecutive reactions. A UV-induced reaction of 1,2-epoxy-9-decene with hydrogen-terminated Si_xN_4 surfaces was followed by conversion of the epoxide with 1,2-ethylenediamine resulting in primary and secondary amine-terminated surfaces. A reaction with 2-bromoisobutyryl bromide led to ATRP initiator-covered surfaces. Zwitterionic polymer brushes of SBMAA were grown from these initiator-coated surfaces (thickness ∼30 nm), and the polymer-coated surfaces were characterized in detail by static water contact angle measurements, X-ray photoelectron spectroscopy (XPS), and an atomic force microscope (AFM). The adsorption of proteins onto zwitterionic polymer coated surfaces was evaluated by *in situ* reflectometry, using a fibrinogen (FIB) solution of 0.1 g·L^{-1}, and compared to hexadecyl-coated Si_xN_4 surfaces (C_{16}−Si_xN_4), uncoated air-based plasma oxidized Si_xN_4 surfaces (SiO_y−Si_xN_4), and hexa(ethylene oxide)-coated Si_xN_4 surfaces (EO_6−Si_xN_4). Excellent protein repellence (>99%) was observed for these zwitterionic polymer-coated Si_xN_4 surfaces during exposure to FIB solution as compared to C_{16}−Si_xN_4 surfaces. Furthermore, the stability of these zwitterionic polymer-coated Si_xN_4 surfaces was surveyed by exposing the surfaces for 1 week to phosphate buffered saline (PBS) solution at room temperature. The zwitterionic polymer-coated Si_xN_4 surfaces before and after exposure to PBS solution were characterized by XPS, AFM, and water contact angle measurements, and their protein-repelling properties were evaluated by reflectometry. After exposure to PBS solution, the zwitterionic polymer coating remained intact, and its thickness was unchanged within experimental error. No hydrolysis was observed for the zwitterionic polymer after 1 week exposure to PBS solution, and the surfaces still repelled 98% FIB as compared to C_{16}−Si_xN_4 surfaces, demonstrating the long-term efficiency of these easily prepared surface coatings.

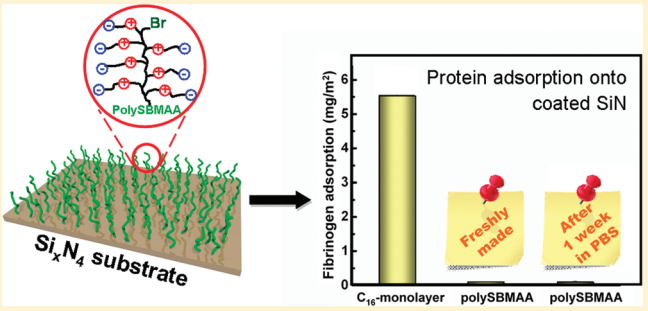

1. INTRODUCTION

Protein-resistant coatings are of paramount importance in many biomedical applications such as contact lenses, biosensors, and prostheses. The adhesion of proteins onto exposed areas of these devices may eventually lead to thrombosis, produce false results in diagnostics, or limit the precision of medical instruments.[1−4] Therefore, minimizing the interactions between proteins and the surfaces is a prerequisite for the long-term use thereof.

Over the past decades, poly- and oligo(ethylene oxide) have been widely used to reduce nonspecific binding of proteins.[5−8] The hydration layer surrounding the ethylene oxide chains due to hydrogen bonding is considered to be the reason for the efficient repulsion of proteins. Protein resistance of poly- or oligo(ethylene oxide) coated to various substrates was demonstrated and corroborated by experimental and simulation studies.[5,6,9−16] However, the ethylene oxide chains are over time auto-oxidized in aqueous solution, resulting in cleavage of ethylene oxide units and formation of aldehyde-terminated chains.[17] These aldehyde moieties may react with proteins bearing amine groups, resulting in a declination of the protein-repellent nature of the coatings.[17] Moreover, the poly(ethylene oxide) coatings lose their protein resistance at 37 °C,[18] which is a critical temperature for many biomedical applications.

Recently, zwitterionic polymer brush coated surfaces have emerged as a superior alternative to poly(ethylene oxide) coatings.[19] The zwitterionic polymers display minimized adhesion of proteins due to a more strongly bound hydration layer induced by electrostatically ionic solvation in addition to hydrogen-bonding interactions. The electrostatic interactions between water molecules and dipoles present in the zwitterionic polymer chains make these polymers better "water-bearers". Moreover, these

Received: November 23, 2010
Revised: December 17, 2010
Published: February 03, 2011

interactions are more stable at body temperature than hydrogen-bonding interactions along an ethylene oxide chain.[20−25]

The growth of zwitterionic polymers from gold,[19,22,26−30] silicon,[24] and also polymer[31] surfaces via surface-initiated atom transfer radical polymerization (ATRP) has been reported. ATRP is a controlled radical polymerization technique that enables the formation of well-defined polymers on the surface. It has found widespread applications due to its relative simplicity and versatility.[32,33] However, coatings on silicon surfaces are typically obtained via silanization resulting in Si−O−Si−C linkages, which are reported to hydrolyze in slightly basic media,[34] and may result in severe detachment of these coatings. Alternative approaches were introduced to immobilize various functional molecules onto silicon[35−37] and silicon nitride[38−40] substrates via Si−C and N−C linkages. These monolayers were demonstrated to possess significant stability in both acidic and basic media.[34,41] We recently investigated the stability of hexa(ethylene oxide) methyl ω-undecenyl ether coated Si_xN_4 surfaces ($EO_6-Si_xN_4$).[42] The initial protein repellence was high (94% for bovine serum albumin), but this value diminished over time (week long exposure to phosphate buffered saline (PBS)). Although no oxidation of the Si_xN_4 surface was observed after exposure to PBS solution, auto-oxidation of the ether moieties in the monolayer still occurred,[42] keeping long-term protein repulsion out of reach.

Si_xN_4 is often used as an insulator and chemical barrier in manufacturing integrated circuits.[43] As a passivation layer for microchips, it is superior to silicon dioxide, as it provides a significantly better diffusion barrier.[44] Nowadays it is widely used in micro- and nanoelectromechanical systems (MEMS and NEMS).[45] Silicon nitride has excellent fracture toughness and is chemically inert, which presents opportunities for micro/nano devices with high corrosion resistance and high mechanical strength, as alternatives to silicon-based devices.[46] Among other possibilities, this enables the fabrication of microsieves with high porosity and highly homogeneous pore-size distributions.[47] Microsieves therefore have a high flux and excellent selectivity in microfractionation processes. They have been applied in many fields, for instance, in biological sample preparation, food processing, emulsification, filtration, atomization, and diagnostics.[48,49]

However, as for any conventional membrane, microsieves also face fouling issues, that is, the nonspecific adsorption of biomolecules on surfaces during filtration. Proteins especially initiate surface contamination[50] and thereby facilitate the growth of thicker biofouling layers, which considerably affects device performance.[51] Therefore, the development of stable protein-resistant coatings on membrane surfaces is needed to minimize fouling and to maintain process capacity.[52]

In this study, we introduce a method to obtain dense monolayers of ATRP initiators coated onto Si_xN_4 surfaces via stable Si−C linkages, which serve as an excellent template for growing polymers. ATRP is employed to graft zwitterionic polymer brushes from the Si_xN_4 surfaces. The polymer-coated surfaces is characterized in detail, and their stability is assessed. Finally, the protein repelling properties are evaluated by long-term (1 week) exposure of the surfaces to fibrinogen solution and following the adsorption by in situ reflectometry, to reveal the long-term potential of zwittterionic polymer coatings as protein-repelling layers.

2. EXPERIMENTAL SECTION

2.1. Materials and Methods. Fibrinogen (fraction I from porcine plasma, 78% in protein) was purchased from Sigma Adrich. Sodium phosphate dibasic (analytical grade, Acros), potassium dihydrogenophosphate (ACS grade, Merck), potassium chloride (pro analysis, Merck), and sodium chloride (puriss, Riedel-de-Haën) were used to prepare the PBS buffer.

1,2-Epoxy-9-decene (96%), 1,2-ethylenediamine (p.a., absolute, ≥99.5%), *n*-propylamine (≥99%), dichloromethane (DCM, 99.8%, extra dry over molecular sieve, stabilized with amylene), acetone (semiconductor grade), copper(I) bromide (99.999%), [3-(methacryloylamino)propyl]dimethyl(3-sulfopropyl)ammonium hydroxide inner salt (SBMAA, 96%), 2,2′-bipyridine (99%), 2-bromoisobutyryl bromide (98%), isopropanol (*i*-PrOH, absolute, 99.9%), and triethylamine (Et_3N) were purchased from Sigma-Aldrich. Petroleum ether 40−60 was distilled before use. All experiments used ultrapure water purified by a Barnsted water purification system with a resistance of 18.3 MΩ·cm. For the formation of epoxide monolayers, 1,2-epoxy-9-decene was purified by column chromatography. The obtained purity was >99% as determined by gas chromatography/mass spectroscopy (GC-MS).

Si_xN_4 ($x > 3$) was deposited on Si ⟨100⟩ substrates (p-type, slightly boron doped, resistance 8−22 Ω·cm) by low-pressure chemical vapor deposition (LPCVD) with a thickness of 150 nm (Nanosens B.V., The Netherlands). The Si_xN_4 wafers were cut into appropriate sizes for each experiment. Si_xN_4 samples were cleaned by dust-free wipers with acetone, followed by oxidation in air-based plasma for 10 min. The oxidized samples were then etched with a 2.5% aqueous solution of HF for 2 min and dried under an argon flow. Immediately the samples were transferred into degassed neat 1,2-epoxy-9-decene in a quartz flask, followed by three vacuum-argon cycles to remove trace amounts of oxygen that might enter the flask during sample transfer. Finally, the flask was backfilled with argon. A UV pen-lamp (254 nm, low pressure mercury vapor, double bore lamp from Jelight Company Inc., California) with the output intensity of 9 mW·cm^{-2} was aligned 4 mm away from the quartz flask. The samples were irradiated under argon for 24 h. The samples were removed from the flask and sonicated in acetone for 5 min, rinsed several times with acetone and distilled petroleum ether, and finally dried in a stream of argon. Subsequently, the samples were transferred to degassed neat 1,2-ethylenediamine. The reaction was carried out for 24 h at 40 °C. The samples were removed from the flask, and the same cleaning procedure was employed as described for the previous experiment. The ATRP initiator was attached onto the amine-terminated surfaces via a reaction with 2-bromoisobutyryl bromide (0.54 g, 2.00 mmol) in dry dichloromethane (1 mL) containing Et_3N (0.2 mL) at room temperature for 30 min. The surfaces were removed and subsequently cleaned by sonication in DCM for 5 min and rinsed thoroughly with acetone and distilled petroleum ether.

The hexadecyl-coated Si_xN_4 surfaces ($C_{16}-Si_xN_4$) and hexa(ethylene oxide)-coated Si_xN_4 surfaces ($EO_6-Si_xN_4$) were prepared via the same procedure as was used for immobilization of 1,2-epoxy-9-decene on Si_xN_4 surfaces as described above. The hexadec-1-ene and methoxy-hexa(ethylene oxide) undec-1-ene were employed to react with hydrogen-terminated surfaces obtained by HF etching. The synthesis and purification of the compounds as well as the characterization of these surfaces are described in detail elsewhere.[42]

2.2. Surface-Initiated Polymerization. Poly(sulfobetaine acrylamide) (SBMAA) (1.20 g, 4.00 mmol) and 2,2′-bipyridine (0.32 g, 2.00 mmol) were dissolved in a mixture of isopropanol (7.5 mL) and water (2.5 mL) in a round-bottomed flask by

Scheme 1. Si_xN_4 Surface Modification Reactions and Surface Initiated Controlled Radical Polymerization

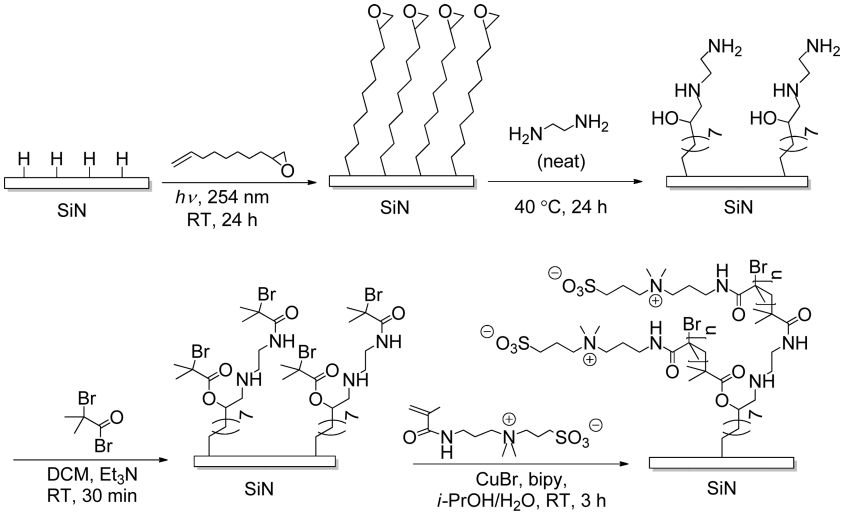

stirring. The solution was degassed for 30 min by purging with argon. CuBr (0.14 g, 1.00 mmol) was added to a separate round-bottomed flask under argon (in a glovebox) which was closed by a septum. Subsequently, the degassed solution was transferred into the flask containing CuBr by means of a syringe (flushed with argon in advance). The mixture was stirred further for an additional 30 min under argon to dissolve all CuBr. Afterward, the mixture was transferred to the reaction flask containing the initiator-coated Si_xN_4 surface by means of a syringe. The polymerization was carried out under argon pressure (0.14 bar overpressure) while stirring at room temperature for 3 h (Scheme 1). The samples were removed and rinsed with warm water (60−65 °C) for 5 min and cleaned by sonication in water and further with acetone. Finally, the samples were dried under a stream of argon.

The thickness of the polySBMAA layer was determined as a function of reaction time. To this purpose the substrate was placed in a special holder equipped with a magnet, which made it possible to move the holder by an external magnet. The degassed polymerization solution prepared as described above was injected into the reaction flask containing the initiator-coated Si_xN_4 surface. Subsequently, the sample holder was submerged partly into the polymerization solution and moved in further in a stepwise manner with several intervals. The polymerization was carried out under argon pressure with agitation for 8 h. Finally, the sample was removed, and the same cleaning procedure was employed as described earlier. Thicknesses of the different areas were determined by atomic force microscopy (AFM).

2.3. Protein Adsorption. Fibrinogen (FIB) solutions (0.1 $g \cdot L^{-1}$) were freshly prepared in PBS solution (phosphate buffered saline; pH 6.7, ionic strength 0.08 M) and settled for 1 h at room temperature before use. Because of the low solubility of FIB in water, FIB solutions were prepared as follows. First, a PBS solution was prepared at pH 6.7 with high ionic strength (0.16 M). Next, the desired amount of FIB was added, and the solution was gently shaken at 80 rpm at room temperature. After 15 min, FIB had completely dissolved, and a clear protein solution was obtained. Finally, the solution was diluted 2 times to obtain 0.1 $g \cdot L^{-1}$ of FIB in PBS solution at pH 6.7 with an ionic strength of 0.08 M. All reflectometry experiments were performed at room temperature. Before measurements, surfaces were incubated for 1 h in warm water (60−65 °C) to sufficiently wet the coatings and subsequently in PBS solution for 1 h to avoid artifacts. Consecutively, after placing the samples in the reflectometer, buffer solution was injected until the output signal remained constant: fluctuations of less than 0.01 V over 5 min were considered satisfactory. Each experiment involved at least one adsorption phase, in which protein solutions was added to the surface, and one desorption phase, in which only buffer was injected. Details on the calculation of adsorbed protein amount have been reported earlier.[42,53]

2.4. Stability of Zwitterionic SBMAA-Coated Si_xN_4 Surfaces in PBS Solution. Three samples of zwitterionic SBMAA-coated Si_xN_4 surfaces were prepared in a single batch as described above. A study on the stability of zwitterionic SBMAA-coated on Si_xN_4 surfaces in PBS solution was performed at room temperature for 1 week. Before and after exposure to PBS solution, the samples were characterized by XPS, their thicknesses were determined by AFM and reflectometry measurements were carried out to evaluate their protein repellency. Static water contact angle measurements were performed daily, after rinsing the samples thoroughly with pure water followed by acetone. The samples were immersed every day in fresh PBS solution. After 1 week of immersion in PBS solution, the samples were rinsed thoroughly with pure water prior to protein adsorption experiments. Afterward, the samples were rinsed thoroughly with 1% sodium dodecyl sulfate in water (SDS) to remove any adsorbed FIB, subsequently with pure water and sonication in water, followed by acetone, before XPS and AFM measurements.

2.5. X-ray Photoelectron Spectroscopy (XPS). Modified surfaces were characterized by XPS using a JPS-9200 photoelectron spectrometer (JEOL, Japan). High-resolution spectra were obtained under UHV conditions using monochromatic Al Kα X-ray radiation at 12 kV and 20 mA, using an analyzer pass energy of 10 eV. All high-resolution spectra were corrected with a linear background before fitting.

2.6. Static Water Contact Angle Measurements. The wettability of the modified surfaces was determined by automated static water contact angle measurements with the use of an Erma contact angle meter G-1 (volume of the drop of demineralized water is 2.5 μL).

2.7. Atomic Force Microscopy (AFM) for Thickness and Roughness Measurements. AFM surface images were measured

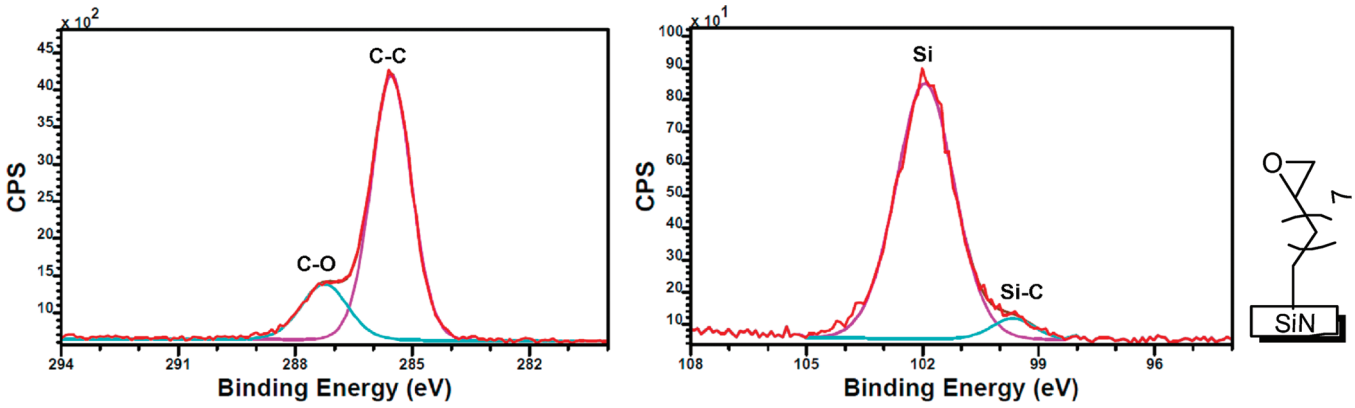

Figure 1. Narrow-scan XPS spectra of C_{1s} region (left) and Si_{2p} (right) region of epoxide-terminated Si_xN_4 surface.

with Tap300Al-G silicon cantilevers (Budgetsensors) in AC mode in air using an Asylum Research MFP-3D SA AFM. Prior to the thickness measurements, surfaces were prepared as follows. The polymer-coated surfaces were immersed in pure water for 4 h at room temperature to fully swell polymer. A knife was used to scratch the surfaces. The scratched surfaces were sonicated to remove any residuals from cutting, and the sample surface was subsequently dried with argon. The scratched surfaces were directly measured by AFM. The thickness of the swollen polymer layer was determined from the height difference in the topography profile. The root-mean-square (rms) roughness was calculated from the topography of the surface.

2.8. Reflectometry. In a reflectometer, a monochromatic linearly polarized light beam (He−Ne laser; 632.8 nm) passes a 45° glass prism. This beam arrives at the interface with an angle of incidence of 66° for the solvent−substrate interface. After reflection at the interface and refraction in the prism, the beam is split into its p- and s-polarized components relative to the plane of incidence by means of a beam splitter. Both components are separately detected by two photodiodes, and the ratio between the intensity of the parallel and perpendicular components is the output signal S ($S = I_p/I_s$) (the output signal given by the detection box is $10 \times S$). It is combined with a stagnation point flow cell, allowing the introduction of buffer or protein solutions, to study homogeneous adsorption on surfaces in diffusion-controlled conditions.[53] Si_xN_4 wafers were cut into small strips with a typical size of 4×0.75 cm and functionalized with SBMAA on one side (about 1 cm from the flange of the sample). The other end was clamped into the measuring cell of the reflectometer.

3. RESULTS AND DISCUSSION

3.1. Formation and Characterization of Monolayers on SiN. *3.1.1. Epoxide-Terminated Monolayer.* Silicon nitride was functionalized in a four-step procedure (Scheme 1). Hydrogen-terminated Si_xN_4 surfaces were obtained through etching with HF and employed in the photochemical attachment of 1,2-epoxy-9-decene.[35,54]

A static water contact angle of 71 ± 1° was observed for the epoxide-terminated Si_xN_4 surface, which is identical to that reported earlier for epoxy-coated silicon surfaces.[54] No signal corresponding to silicon oxide was observed in the narrow-scan XPS spectrum of Si_{2p} region (Figure 1, right). The narrow-scan XPS spectrum of C_{1s} region displays a peak at 287.0 eV corresponding to carbon atoms bound to oxygen (C−O) derived from the epoxide moiety and a peak at 285.0 eV corresponding to carbon bound to carbon (C−C) which results from the alkyl chain (Figure 1, left). The ratio of (C−C)/(C−O) is 4.0, that is, in excellent agreement with the theoretical composition. These results indicate that high-quality epoxide monolayers on Si_xN_4 were obtained.

3.1.2. Amine-Terminated Monolayer. The epoxide-terminated Si_xN_4 surface was subsequently converted into an amine-terminated surface via a reaction with neat 1,2-ethylenediamine under argon (Scheme 1). The static water contact angle decreased from 71 ± 1° to 63 ± 1°, which is in good agreement with earlier reported amine-terminated monolayers on silicon.[55] A 1 eV shift of the C−O peak was observed in the narrow-scan XPS spectrum of the C_{1s} region corresponding to epoxide ring-opening and attachment of the amine moiety. A broad C_{1s} peak at 286 eV is attributed to the overlapping signals of C−O (from secondary alcohol) and C−N in the resultant monolayer (Figure 2, left). The experimental ratio of C−C/(C−O and C−N) is 2.1, which corresponds to the attachment of 1,2-ethylenediamine onto the epoxide-terminated surface via a single amine moiety (theoretically expected ratio: 2.0). Bridged conformations, in which a single 1,2-ethylenediamine molecule is coupled to two epoxide moieties, would have resulted in a significantly higher ratio (2.6), while unreacted epoxide moieties would give a ratio of 4.0. In addition, a signal of organic nitrogen at 399 eV from the resultant monolayer appears next to a signal of inorganic nitrogen at 397 eV (Figure 2, right), which further demonstrates the successful attachment of 1,2-ethylenediamine onto the epoxide-terminated Si_xN_4 surface. The narrow-scan XPS spectrum of C_{1s} region reveals a high conversion of the epoxides (95%) (see Supporting Information). The strategy shown here provides a new route to obtain amine-terminated Si_xN_4 surfaces via stable Si−C linkages without the need for protective group chemistry[56,57] or the use of silane chemistry involving the hydrolytically labile Si−O linkages.

3.1.3. Br-Initiator-Functional Monolayer. ATRP initiators were attached to the amine-terminated surfaces via a reaction with 2-bromoisobutyryl bromide (Scheme 1). The water contact angle of the modified surfaces was 72 ± 1°, which is very close to those observed for similar monolayers on gold (73°).[58] The appearance of characteristic bromine-signals (Br_{3d} at 70 eV, Br_{3s} at 255 eV, and Br_{3p} at 188 eV) was observed in the wide-scan XPS spectrum (data not shown). The C_{1s} peak at 288.3 eV corresponds to an amide-carbonyl C atom in the resultant monolayer,

dx.doi.org/10.1021/la104657c |*Langmuir* 2011, 27, 2587–2594

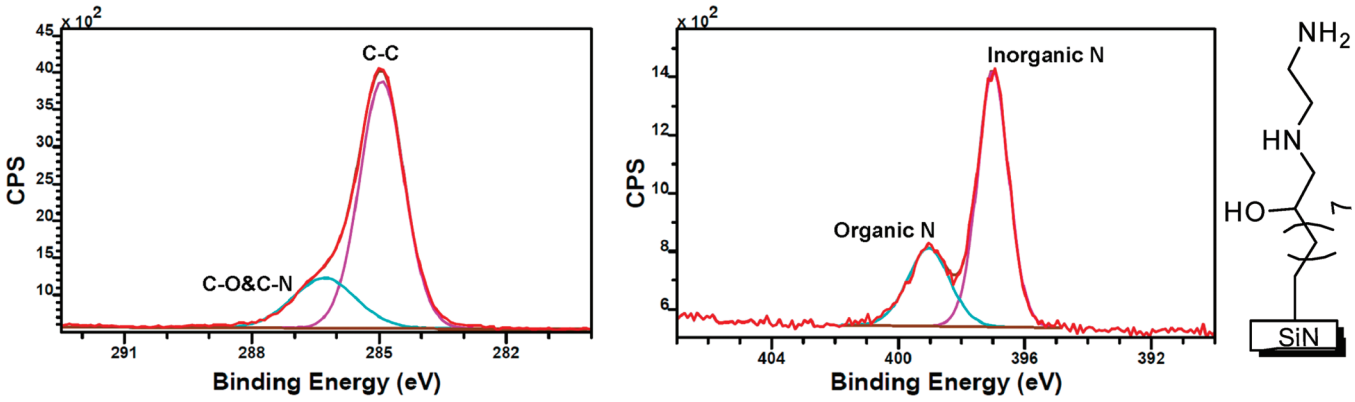

Figure 2. Narrow-scan XPS spectra of C_{1s} region (left) and N_{1s} (right) region of amine-terminated Si_xN_4 surface.

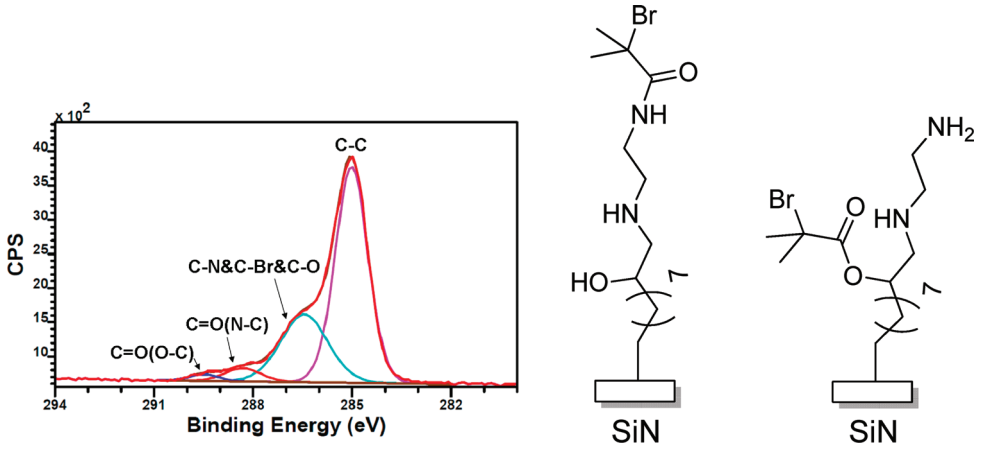

Figure 3. Narrow-scan XPS spectrum of C_{1s} region of Br-initiators terminated Si_xN_4 surface.

whereas the peak at 289.5 eV corresponds to the ester-carbonyl moiety. This indicates that not only the amines participate in the coupling reaction, but the secondary alcohol that resulted from the original epoxide-ring-opening as well (Figure 3). The broad peak at 286.5 eV is attributed to overlapping C−N, C−Br, and C−O(C═O) peaks.

To determine to what extent the secondary alcohol and secondary amine participate in the reaction with 2-bromoisobutyryl bromide, an epoxide-terminated surface was reacted with *n*-propylamine instead of 1,2-ethylenediamine. This results in an *n*-propyl-terminated surface that presents a secondary alcohol and a secondary amine. The resultant surface was reacted with 2-bromoisobutyryl bromide. In this case, the narrow-scan XPS spectrum of C_{1s} of the Br-initiator-coated surface shows approximately 40% conversion of secondary alcohols into ester moieties and 30% secondary amide formation. This low conversion is attributed to the sterically hindered positions of the secondary alcohol and the secondary amine in the monolayer (see Supporting Information). In the case of amine-terminated surfaces stemming from the 1,2-ethylenediamine reaction, carried out under water-free conditions, roughly 30% conversion was observed for the secondary alcohol and approximately 70% conversion of primary or secondary amine into amide moieties (see Supporting Information). These results show a high overall conversion (∼100%) for the attachment of Br-initiators, with respect to each alkyl chain, hence providing an excellent template for growing dense polymeric coatings.

3.2. Surface-Initiated Polymerization. PolySBMAA was grafted from the Br-initiator coated Si_xN_4 surfaces via ATRP (Scheme 1). After polymerization, the water contact angle values of the modified surfaces were below the detection limit of the equipment (<15°), which is in agreement with earlier observations for similar polymer-coated gold surfaces.[22,28−30] The wide-scan XPS spectrum of the SBMAA-grafted Si_xN_4 surface no longer displays a signal of silicon at 102 eV, demonstrating the presence of a thick polymer layer coated on the substrate (Figure 4). Furthermore, the wide-scan XPS spectrum showed the presence of oxygen (20%), carbon (65%), nitrogen (10%), and sulfur (5%), with an elemental composition in agreement with the composition of the SBMAA monomeric unit. The narrow-scan XPS spectrum of the N_{1s} region revealed two distinct peaks for nitrogen, one for nitrogen atoms corresponding to amide, and the other signal stemming from the quaternary amine in the monomer. The roughness of the polySBMAA-grafted surfaces measured by AFM was 1.5 ± 0.1 nm, demonstrating the presence of a smooth polySBMAA layer. The thickness of the polySBMAA layer was measured by AFM, by comparing it with an area where the polymer layer was removed. A kinetics study was performed, and the polymer film thicknesses were determined as a function of reaction time as shown in Figure 5. A high initial polymerization rate was observed, after which the thickness increased approximately linear with time at a rate of ∼6 nm/h. These data demonstrate that polySBMAA was grafted successfully from the initiator-coated Si_xN_4 surface in a controlled way.

dx.doi.org/10.1021/la104657c |*Langmuir* 2011, 27, 2587–2594

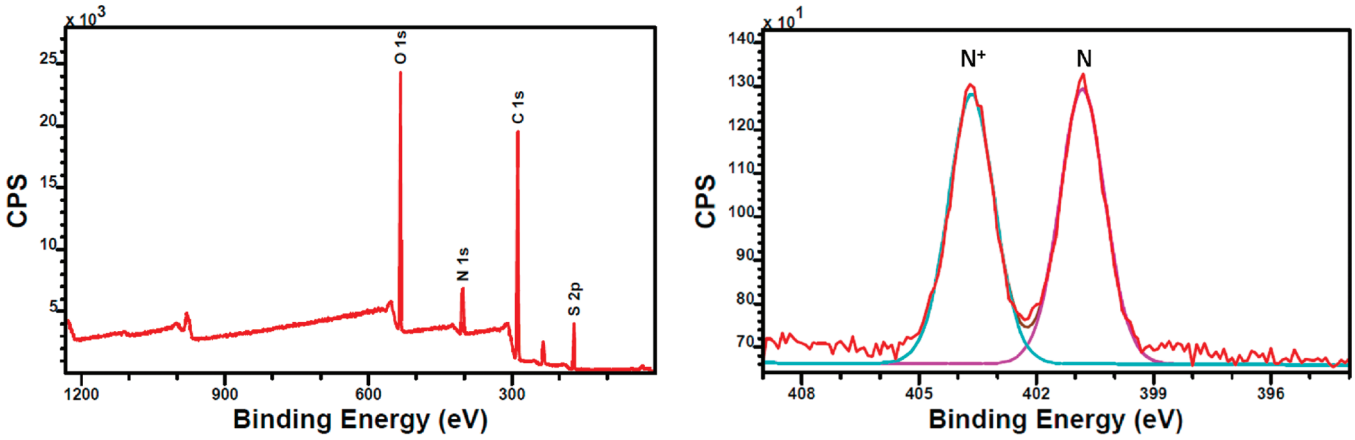

Figure 4. Wide-scan XPS spectrum (left) and narrow-scan XPS spectrum of N_{1s} (right) region of polySBMAA-grafted Si_xN_4 surface.

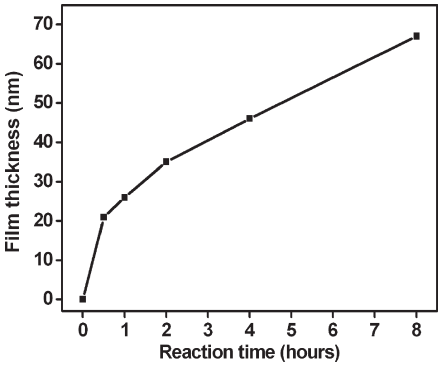

Figure 5. Thickness of polySBMAA grafted from Si_xN_4 as a function of reaction time.

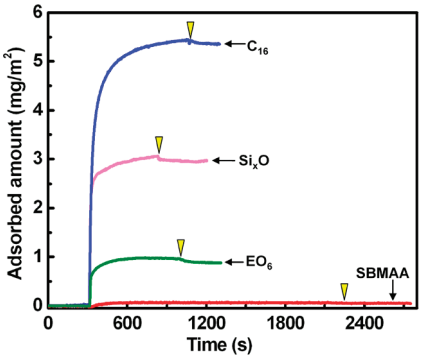

Figure 6. FIB adsorption onto the modified Si_xN_4 surface (yellow arrows indicate the desorption transition).

3.3. Protein Adsorption Experiments. The protein-repelling properties of the obtained polySBMAA-grafted Si_xN_4 surfaces (polymer thickness of 34 ± 2 nm) were evaluated by reflectometry measurements and compared with several commonly employed substrates. The use of reflectometry in studying protein adsorption enables us to examine real-time changes in the refractive index of the surfaces and thereby reveals both reversible and irreversible adsorption stages.[42] Upon employing the surfaces coated with zwitterionic polymers in a protein adsorption experiment, minimal adsorption of FIB was observed (0.06 mg·m^{-2}). This result is in good agreement with the resultant protein repellence of zwitterionic polymer coated on gold[19,22,26−30] and silicon[24] surfaces. When exposed to FIB solution, the $C_{16}-Si_xN_4$ surface (hydrophobic surface) rapidly adsorbed protein; a maximum adsorbed amount of 5.5 mg·m^{-2} was found (Figure 6). Such behavior was reported earlier for similar hydrophobic coatings, that is, alkyl coatings on gold[59] and silicon.[60] Hydrophobic surfaces generally have a very low surface energy, and as a result proteins readily adsorb to minimize the interfacial tension between the surface coating and the water.[61] In comparison, the plasma-oxidized $Si_yO-Si_xN_4$ surface (hydrophilic surface) adsorbed only 3.1 mg·m^{-2}, that is, 44% protein repulsion as compared to the $C_{16}-Si_xN_4$ surface. Hydrophilic surfaces, such as $Si_yO-Si_xN_4$, generally have much higher surface energy and only low interfacial energy when in contact with water. Thermodynamically, it is not favorable for proteins to adsorb onto the surface. Therefore, many hydrophilic surfaces are known to repel proteins. However, surface hydrophilicity plays only a minor role in protein repulsion. Indeed, Figure 6 shows that the $EO_6-Si_xN_4$ surface (a typical well-performing antifouling surface) has a water contact angle of 62°, which is thus significantly less hydrophilic than the $Si_yO-Si_xN_4$ surface (CA < 5°). Nevertheless, $EO_6-Si_xN_4$ adsorbed only 0.96 mg·m^{-2}; in other words 83% of FIB was repelled from the modified surface as compared to a $C_{16}-Si_xN_4$ surface. The ethylene oxide moieties inside the EO_6 monolayer are able to form hydrogen bonds with water molecules and consequently maintain a persistent hydration layer. This generates a repulsive force which makes it difficult for proteins to reach the surface.[14−16] The $SiO_y-Si_xN_4$ surface has a hydration layer of only a few water molecules. Thus, the water molecules are easily pushed away by approaching proteins. Hence, an effective antifouling coating must be able to maintain a persistent hydration layer; that is, a good hydration layer should have a strong inherent interaction between water and the coatings and a thick layer of hydration. These factors play a crucial role in the protein repulsion effectiveness of the surfaces.[20] Zwitterionic polymer brushes are significantly more effective (99%) in repelling FIB as compared to EO_6 monolayers (87%) and SiO_y (44%) due to an increased hydration layer (all compared to C_{16}−alkyl monolayers as reference).

3.4. Stability of Zwitterionic SBMAA Coated on Si_xN_4 Surfaces in PBS Solution. To study the stability of the polySBMAA coated on Si_xN_4 surfaces in an aqueous medium, the samples were immersed in PBS solution and characterized before and after a 1-week exposure. The water contact angle values remained lower than 15° throughout the experiment. The wide-scan XPS spectrum

shows minor signals of silicon (<1.5% on average for three samples) after immersion in PBS solution for 1 week, indicating that the zwitterionic polymeric coating was still intact. In addition, the narrow-scan XPS spectrum of C_{1s} region showed the same elemental composition for the exposed surfaces as observed for the fresh samples, showing no hydrolysis or degradation of the zwitterionic polymer (Supporting Information). The thickness measured by AFM remained unchanged within the error of measurement and further confirms that no significant polymer detachment occurred. The integrity of the polymeric coating was further verified by again measuring its protein-repellent behavior. The adsorbed amount of FIB on the exposed surfaces was still only 0.12 ± 0.02 mg·m^{-2}; that is, the surfaces still repel 98% of FIB as compared to the $C_{16}-Si_xN_4$ surface.

4. CONCLUSIONS

SBMAA zwitterionic polymer brushes were successfully grafted from Si_xN_4 surfaces. The use of functional monolayers on Si_xN_4 served as an excellent template for polymer grafting as well as providing stability to the polymer coating. The SBMAA zwitterionic polymer brushes grafted on Si_xN_4 surfaces show excellent antifouling behavior in FIB solution as compared to hydrophobic $C_{16}-Si_xN_4$ surfaces (>99% repulsion) and other commonly applied protein-repelling surfaces. After exposure to PBS solution for 1 week, the surfaces still repelled 98% FIB as compared to the $C_{16}-Si_xN_4$ surface, while the polymeric coating remained intact. The inertness of the silicon nitride substrate and the robust Si−C linkage through which the zwitterionic polymers are coupled provide for highly stable and effective antifouling surfaces, greatly contributing to the development of long-term use biological devices such as in membrane filters, microreactors, biosensors, and medical instruments in general.

■ ASSOCIATED CONTENT

Supporting Information. The calculations of the conversion of modified surfaces and AFM image of polySBMAA-grafted Si_xN_4 surface. This material is available free of charge via the Internet at http://pubs.acs.org.

■ AUTHOR INFORMATION

Corresponding Author

*E-mail: Han.Zuilhof@wur.nl. Phone: +31-317-482361.
jacobbaggerman@aquamarijn.nl. Phone: +31-575-519731.

■ ACKNOWLEDGMENT

The authors thank MicroNed (project 6163510587) for financial support and Hien Duy Tong (Nanosens B.V., Zutphen, The Netherlands) for his kind donation of Si_xN_4 wafers.

■ REFERENCES

(1) Desai, T. A.; Hansford, D. J.; Leoni, L.; Essenpreis, M.; Ferrari, M. *Biosens. Bioelectron.* **2000**, *15*, 453–462.
(2) Mandrusov, E.; Puszkin, E.; Vroman, L.; Leonard, E. F. *ASAIO J.* **1996**, *42*, M506–513.
(3) Sampedro, M. F.; Patel, R. *Infect. Dis. Clin. North. Am.* **2007**, *21*, 785–819.
(4) Turner, R. F. B.; Harrison, D. J.; Rojotte, R. V. *Biomaterials* **1991**, *12*, 361–368.
(5) Roosjen, A.; van der Mei, H. C.; Busscher, H. J.; Norde, W. *Langmuir* **2004**, *20*, 10949–10955.
(6) Roosjen, A.; Kaper, H. J.; van der Mei, H. C.; Norde, W.; Busscher, H. J. *Microbiology* **2003**, *149*, 3239–3246.
(7) Roosjen, A.; de Vries, J.; van der Mei, H. C.; Norde, W.; Busscher, H. J. *J. Biomed. Mater. Res., Part B* **2005**, *73*, 347–354.
(8) Norde, W. *Surface Chemistry in Biomedical and Environmental Science*; Blitz, J., Gun'ko, V., Norde, W., Eds.; Springer: Netherlands, 2006; pp 159−176.
(9) Harder, P.; Grunze, M.; Dahint, R.; Whitesides, G. M.; Laibinis, P. E. *J. Phys. Chem. B* **1998**, *102*, 426–436.
(10) Palegrosdemange, C.; Simon, E. S.; Prime, K. L.; Whitesides, G. M. *J. Am. Chem. Soc.* **1991**, *113*, 12–20.
(11) Schlapak, R.; Pammer, P.; Armitage, D.; Zhu, R.; Hinterdorfer, P.; Vaupel, M.; Fruhwirth, T.; Howorka, S. *Langmuir* **2006**, *22*, 277–285.
(12) Sharma, S.; Johnson, R. W.; Desai, T. A. *Langmuir* **2004**, *20*, 348–356.
(13) Sofia, S. J.; Premnath, V.; Merrill, E. W. *Macromolecules* **1998**, *31*, 5059–5070.
(14) Zheng, J.; Li, L. Y.; Chen, S. F.; Jiang, S. Y. *Langmuir* **2004**, *20*, 8931–8938.
(15) Zheng, J.; Li, L. Y.; Tsao, H. K.; Sheng, Y. J.; Chen, S. F.; Jiang, S. Y. *Biophys. J.* **2005**, *89*, 158–166.
(16) Zolk, M.; Eisert, F.; Pipper, J.; Herrwerth, S.; Eck, W.; Buck, M.; Grunze, M. *Langmuir* **2000**, *16*, 5849–5852.
(17) Qin, G.; Cai, C. *Chem. Commun.* **2009**, 5112–4.
(18) Leckband, D.; Sheth, S.; Halperin, A. *J. Biomater. Sci., Polym. Ed.* **1999**, *10*, 1125–1147.
(19) Jiang, S.; Cao, Z. *Adv. Mater.* **2010**, *22*, 920–932.
(20) He, Y.; Hower, J.; Chen, S.; Bernards, M. T.; Chang, Y.; Jiang, S. *Langmuir* **2008**, *24*, 10358–10364.
(21) Holmlin, R. E.; Chen, X.; Chapman, R. G.; Takayama, S.; Whitesides, G. M. *Langmuir* **2001**, *17*, 2841–2850.
(22) Ladd, J.; Zhang, Z.; Chen, S.; Hower, J. C.; Jiang, S. *Biomacromolecules* **2008**, *9*, 1357–1361.
(23) Yang, W.; Xue, H.; Li, W.; Zhang, J.; Jiang, S. *Langmuir* **2009**, *25*, 11911–11916.
(24) Zhang, Z.; Chao, T.; Chen, S.; Jiang, S. *Langmuir* **2006**, *22*, 10072–10077.
(25) Zhao, C.; Li, L.; Zheng, J. *Langmuir* **2010**, *26*, 17375–17382.
(26) Chang, Y.; Chen, W.-Y.; Yandi, W.; Shih, Y.-J.; Chu, W.-L.; Liu, Y.-L.; Chu, C.-W.; Ruaan, R.-C.; Higuchi, A. *Biomacromolecules* **2009**, *10*, 2092–2100.
(27) Chang, Y.; Shu, S.-H.; Shih, Y.-J.; Chu, C.-W.; Ruaan, R.-C.; Chen, W.-Y. *Langmuir* **2009**, *26*, 3522–3530.
(28) Cheng, N.; Brown, A. A.; Azzaroni, O.; Huck, W. T. S. *Macromolecules* **2008**, *41*, 6317–6321.
(29) Omar, A.; Andrew, A. B.; Huck, W. T. S. *Angew. Chem., Int. Ed.* **2006**, *45*, 1770–1774.
(30) Rodriguez Emmenegger, C.; Brynda, E.; Riedel, T.; Sedlakova, Z.; Houska, M.; Alles, A. B. *Langmuir* **2009**, *25*, 6328–6333.
(31) Zhou, M.; Liu, H.; Kilduff, J. E.; Langer, R.; Anderson, D. G.; Belfort, G. *Environ. Sci. Technol.* **2009**, *43*, 3865–3871.
(32) Ohno, K.; Kayama, Y.; Ladmiral, V.; Fukuda, T.; Tsujii, Y. *Macromolecules* **2010**, *43*, 5569–5574.
(33) Matyjaszewski, K.; Xia, J. *Chem. Rev.* **2001**, *101*, 2921–2990.
(34) Sano, H.; Maeda, H.; Ichii, T.; Murase, K.; Noda, K.; Matsushige, K.; Sugimura, H. *Langmuir* **2009**, *25*, 5516–5525.
(35) de Smet, L. C. P. M.; Pukin, A. V.; Sun, Q.-Y.; Eves, B. J.; Lopinski, G. P.; Visser, G. M.; Zuilhof, H.; Sudhölter, E. J. R. *Appl. Surf. Sci.* **2005**, *252*, 24–30.
(36) Effenberger, F.; Gotz, G.; Bidlingmaier, B.; Wezstein, M. *Angew. Chem., Int. Ed.* **1998**, *37*, 2462–2464.
(37) Stewart, M. P.; Buriak, J. M. *Angew. Chem., Int. Ed.* **1998**, *37*, 3257–3260.
(38) Rosso, M.; Giesbers, M.; Arafat, A.; Sudhölter, K.; Zuilhof, H. *Langmuir* **2009**, *25*, 2172–2180.

(39) Coffinier, Y.; Boukherroub, R.; Wallart, X.; Nys, J. P.; Durand, J. O.; Stievenard, D.; Grandidier, B. *Surf. Sci.* **2007**, *601*, 5492–5498.
(40) Arafat, A.; Schroën, K.; de Smet, L.; Sudhölter, E. J. R.; Zuilhof, H. *J. Am. Chem. Soc.* **2004**, *126*, 8600–8601.
(41) Scheres, L.; Arafat, A.; Zuilhof, H. *Langmuir* **2007**, *23*, 8343–8346.
(42) Rosso, M.; Nguyen, A. T.; de Jong, E.; Baggerman, J.; Paulusse, J. M. J.; Giesbers, M.; Fokkink, R. G.; Norde, W.; Schroën, K.; van Rijn, C. J. M.; Zuilhof, H. *ACS Appl. Mater. Interfaces* **2011**, in press (manuscript number: am-2010-00985c.R1).
(43) Bermudez, V. M.; Perkins, F. K. *Appl. Surf. Sci.* **2004**, *235*, 406–419.
(44) Rathi, V. K.; Gupta, M.; Agnihotri, O. P. *Microelectron. J.* **1995**, *26*, 563.
(45) Patil, L. S.; Pandey, R. K.; Bang, J. P.; Gaikwad, S. A.; Gautam, D. K. *Opt. Mater.* **2005**, *27*, 663–670.
(46) Antsiferov, V. N.; Gilev, V. G.; Karmanov, V. I. *Refract. Ind. Ceram.* **2003**, *44*, 108–114.
(47) van Rijn, C. J. M. *Nano and Micro Engineered Membrane Technology*; Elsevier: Amsterdam, The Netherlands, 2004.
(48) Girones, M.; Bolhuis-Versteeg, L.; Lammertink, R.; Wessling, M. *J. Colloid Interface Sci.* **2006**, *299*, 831–840.
(49) Wagdare, N. A.; Marcelis, A. T. M.; Ho, O. B.; Boom, R. M.; van Rijn, C. J. M. *J. Membr. Sci.* **2010**, *347*, 1–7.
(50) Norde, W. *Adv. Colloid Interface Sci.* **1986**, *25*, 267–340.
(51) Marshall, A. D.; Munro, P. A.; Tragardh, G. *Desalination* **1993**, *91*, 65–108.
(52) Rosso, M.; Schroën, K.; Zuilhof, H. *New Membranes and Advanced Materials for Wastewater Treatment*; American Chemical Society: Washington, DC, 2009; Vol. 1022, pp 151−163.
(53) Dijt, J. C.; Cohen Stuart, M. A.; Fleer, G. J. *Adv. Colloid Interface Sci.* **1994**, *50*, 79–101.
(54) Böcking, T.; Kilian, K. A.; Gaus, K.; Gooding, J. J. *Langmuir* **2006**, *22*, 3494–3496.
(55) Balachander, N.; Sukenik, C. N. *Langmuir* **1990**, *6*, 1621–1627.
(56) Arafat, A.; Giesbers, M.; Rosso, M.; Sudhölter, E. J. R.; Schroën, K.; White, R. G.; Yang, L.; Linford, M. R.; Zuilhof, H. *Langmuir* **2007**, *23*, 6233–6244.
(57) Sieval, A. B.; Linke, R.; Heij, G.; Meijer, G.; Zuilhof, H.; Sudhölter, E. J. R. *Langmuir* **2001**, *17*, 7554–7559.
(58) Jones, D. M.; Brown, A. A.; Huck, W. T. S. *Langmuir* **2002**, *18*, 1265–1269.
(59) Herrwerth, S.; Eck, W.; Reinhardt, S.; Grunze, M. *J. Am. Chem. Soc.* **2003**, *125*, 9359–9366.
(60) Yam, C. M.; Lopez-Romero, J. M.; Gu, J. H.; Cai, C. Z. *Chem. Commun.* **2004**, 2510–2511.
(61) Krishnan, S.; Weinman, C. J.; Ober, C. K. *J. Mater. Chem.* **2008**, *18*, 3405–3413.